nature communications

Article

https://doi.org/10.1038/s41467-026-73630-y

Rethinking the economics and flexibility of U.S. nuclear power through hydrogen integration and policy support

Received: 29 September 2025

Accepted: 13 May 2026

Published online: 02 June 2026

Check for updates

Honglin Li[1,2,3], Jianqiao Huang[3], Bikash Poudel[3], Mucun Sun[3], Tyler Westover[3], Daniel Wendt[3] & Jie Zhang[1,2,4]

Nuclear power supplies reliable low-carbon electricity and high-temperature heat, but existing plants face growing pressure to operate more flexibly in markets with rising renewable penetration. Coupling nuclear reactors with hydrogen production through high-temperature electrolysis may improve flexibility and create additional value, yet its economic potential remains uncertain. Here we show that integrating nuclear generation with hydrogen production and ancillary service participation can substantially improve the economics and operational flexibility of nuclear energy systems. Using an hourly optimization model linked to lifecycle techno-economic analysis, we find that retrofitting existing reactors with high-temperature electrolysis increases average net present value from about -$1.06 billion to about $240 million without policy support, while expanding flexible output by more than 115 MW for most reactors. Policy incentives, cost reductions, and optimized market participation further strengthen the value of nuclear-hydrogen systems for reducing costs and supporting grid reliability.

Nuclear power, as a high-energy-density and highly reliable energy source, has historically played a vital role in providing firm baseload electricity and enhancing energy security[1–3]. Expanding its share can therefore contribute substantially to the stability and resilience of national energy systems[4,5]. Although past concerns over the economic viability of existing nuclear plants in competitive markets have eased in recent years, the rapid transition toward high-penetration renewable energy systems continues to reshape operational requirements for nuclear generation, particularly the need to provide greater flexibility while maintaining cost competitiveness[6–8].

In today's United States (U.S.) power markets, new large nuclear units face steep overnight capital costs ($6000-$12,000 kW^{-1}) and long development timelines, even as electricity systems become more dynamic and price-volatile[9–12]. At the same time, demand for firm, 24/7 supply is rising, partly due to data-center growth, and is leading to higher regional load forecasts and renewed interest in long-term procurement of dependable capacity by utilities and large offtakers[13–15]. These countervailing forces mean that conventional baseload operation remains economically viable in many contexts, especially with policy support for the existing fleet, but also that there is a growing opportunity for nuclear to augment its role through flexible configurations that can capture additional market and system value where merchant exposure is material[16,17].

While the development of next-generation nuclear technologies continues, there is significant yet underexplored potential for retrofitting existing reactors[18]. Nevertheless, the economic and technical feasibility of such retrofits remains uncertain and highly context-dependent[7,19]. Underpinned by policy support, technology readiness, and electricity market conditions, a systematic evaluation of the economic viability, operational flexibility, and integration potential of nuclear plants is urgently needed to inform the future role of nuclear power in the evolving energy landscape[9,20,21] (Fig. 1a, b).

[1]Department of Mechanical Engineering, The University of Texas at Dallas, Richardson, TX, USA. [2]Center for Wind Energy, The University of Texas at Dallas, Richardson, TX, USA. [3]Idaho National Laboratory, Idaho Falls, ID, USA. [4]Department of Electrical and Computer Engineering, The University of Texas at Dallas, Richardson, TX, USA. e-mail: jiezhang@utdallas.edu

As the role of nuclear power undergoes global reconfiguration, national contexts exhibit diverging trajectories and challenges[22,23]. In the U.S., home to the world's largest installed nuclear capacity, nuclear power stands at a critical inflection point, facing pronounced concerns over cost competitiveness and system flexibility[24,25]. The U.S. fleet currently comprises 93 operating reactors, contributing approximately 18% of national electricity generation[26–28]. Yet, the increasing penetration of subsidized renewable generation, despite its variable availability, exerts significant downward pressure on electricity prices, rendering traditional baseload nuclear operations economically unsustainable[10]. Over the past decade, more than a dozen nuclear units have been prematurely retired, and new construction remains limited: aside from the recent connection of Vogtle Units 3 and 4 in Georgia, no new commercial nuclear units have come online in the last 15 years[29,30]. Furthermore, limited ramping capability constrains the role of existing nuclear plants in systems with high shares of variable renewables. In this context, integrating hydrogen production technologies such as low- or high-temperature electrolysis (L/HTE) into existing nuclear plants emerges as a promising approach[31]. This strategy not only allows nuclear units to operate more flexibly by shifting output toward hydrogen production during low-price or low-demand periods, but also creates new revenue streams from hydrogen sales for industrial and transport applications, while enabling cross-sectoral solutions to energy adequacy challenges. Several pilot projects supported by the U.S. Department of Energy, including Nine Mile Point, Palo Verde, and Davis-Besse, explore the coupled nuclear-hydrogen pathway, reflecting continuing policy and industry interest[32–34]. Concurrently, the U.S. government announces ambitious expansion targets: an additional 35 GW of nuclear capacity by 2035 and 200 GW or more by 2050[35]. Achieving these targets requires not only the deployment of advanced and small modular reactors (SMRs), but also the lifetime extension, retrofit, and integration of existing plants with emerging technologies[36,37]. A robust techno-economic assessment of nuclear-hydrogen hybrid systems, accounting for market structures, policy incentives, and regional resource conditions, is therefore essential to determine their feasibility, cost-effectiveness, and deployment value (Fig. 1c, d).

To address these challenges, this study presents a system-level techno-economic assessment of integrating electrolysis-based hydrogen production into existing U.S. nuclear power plants (NPPs)[38]. This approach evaluates the potential of nuclear-hydrogen hybrid systems to enhance operational flexibility and expand revenue opportunities. Focusing on the seven major U.S. independent system operators (ISOs), which feature heterogeneous electricity price structures and ancillary service market designs, the analysis quantifies how regional market mechanisms affect the economic performance of nuclear-hydrogen systems[39–45]. The dispatch model incorporates key operational constraints, including ramping limits, start-up costs, variable efficiency, and part-load performance[21,46]. Hourly simulations characterize power allocation between electricity sales, hydrogen production, and grid service provision. The analysis compares the financial outcomes of baseline (business-as-usual) operations against retrofit and new-build hybrid configurations, evaluating differences across 60- and 80-year plant lifetimes[47]. Results include the breakdown of revenue sources (electricity, hydrogen, ancillary services), estimates of levelized costs (energy and hydrogen), and the cost composition of hydrogen production. In addition, the study explores how policy incentives such as investment and production tax credits affect system profitability and deployment feasibility across diverse market contexts, providing quantitative decision support for regional nuclear-hydrogen integration strategies (Fig. 2).

Results

Economics and revenue diversity of nuclear-hydrogen systems

In the U.S., wholesale electricity is traded through regional markets that are operated by ISOs. ISOs are responsible for maintaining real-time system balance and reliability, while also clearing and settling competitive wholesale markets. In practice, they run an energy market (typically day-ahead and real-time) in which generators are dispatched and compensated based on locational marginal prices (LMPs), and they also procure ancillary services (e.g., regulation and operating reserves) that provide short-term balancing and contingency response. In addition, resource adequacy can be supported through forward capacity mechanisms in some regions (Pennsylvania-New Jersey-Maryland Interconnection (PJM), Independent System Operator New England (ISO-NE), and New York Independent System Operator (NYISO)), whereas others rely primarily on energy-only or alternative adequacy constructs (Electric Reliability Council of Texas (ERCOT), Midcontinent Independent System Operator (MISO), Southwest Power Pool (SPP) and California Independent System Operator (CAISO)). Given this heterogeneity, our analysis focuses on the market components that directly govern short-term dispatch and value-stacking opportunities, namely the energy and ancillary service markets, while treating capacity-related considerations as part of the broader regional context.

Against this market background, we analyzed 42 nuclear reactors from the 93 operating commercial units in the U.S., selecting those with over 10 years of remaining operational lifetime across all seven major ISO regions[38]. Each unit was modeled with integrated high-temperature electrolysis and optional energy storage, with hourly dispatch optimized under representative market conditions. The resulting operational strategies formed the basis for a discounted cash flow Techno-Economic Analysis (TEA) under four scenarios: baseline operation (Case 1), retrofit with hydrogen and storage systems (Case 2), new-build integrated systems (Case 3), and lifecycle/policy comparisons (Case 4). This section examines the economic viability of existing nuclear assets and the incremental value introduced by hydrogen integration.

Conventional nuclear plants, operating as inflexible baseload resources under current electricity market structures, face significant economic headwinds. In Case 1, 41 of the 42 reactors exhibit negative net present values (NPVs) over their remaining lifetimes, with an average deficit of $1.06 billion. While the production tax credit (PTC) (45U) improves the average NPV by $740 million, more than half of the units remain unprofitable. These findings indicate that federal incentives, though beneficial, do not address the fundamental structural limitations. Without enhanced flexibility or diversified revenue streams, conventional nuclear facilities are unlikely to achieve financial self-sufficiency (Fig. 3a).

Retrofit configurations with hydrogen systems (Case 2) mark a pivotal economic shift. A majority of units (61.9%) achieve positive NPVs even in the absence of subsidies, with the average NPV rising to $240 million and a mean internal rate of return (IRR) of 10.2%. Twenty-four reactors achieve payback within four years, reflecting both commercial viability and investment stability. Post-retrofit, average annual revenues reach $510 million, with contributions from hydrogen sales and ancillary service markets. Ancillary service revenues, averaging $12.3 million annually (approximately 2.4% of total revenue), demonstrate how flexible dispatch enables nuclear plants to capture value during periods of low wholesale energy prices. These results underscore that hydrogen-enabled flexibility enhances asset utilization while establishing a compounding value mechanism anchored in market-responsive operations (Fig. 3b).

Federal incentives further enhance financial viability across scenarios. In Case 2, the 45U credit, in addition to increasing the average NPV by $740 million, further reduces payback periods to under two years and substantially improves project bankability. In new-build cases (Case 3 and 4), Clean Electricity PTC (45Y) and Clean Electricity Investment Tax Credit (ITC) (48E) reduce the levelized cost of hydrogen (LCOH) from $22.2 kg^{-1} to $16.0 kg^{-1}, narrowing financial gaps even as NPVs remain negative. Extending system lifetimes from 60 to 80 years reduces the LCOH by approximately $0.15 kg^{-1} but further

https://doi.org/10.1038/s41467-026-73630-y

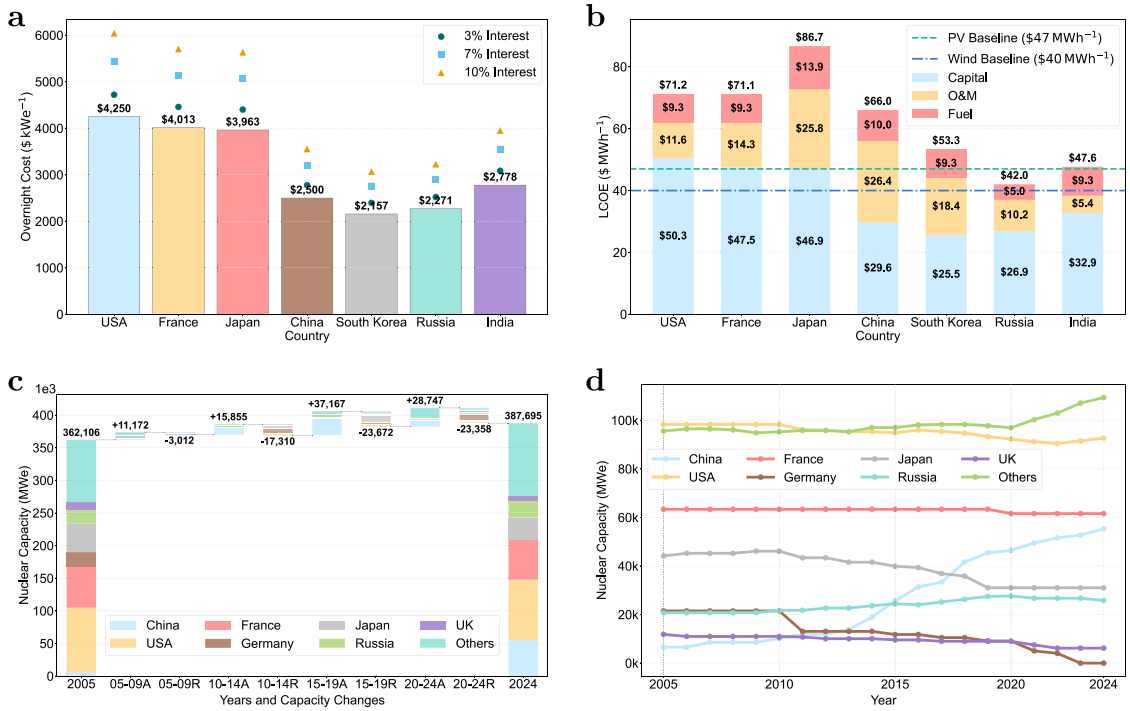


Fig. 1 | Installed capacity and costs of commercial nuclear power across countries. a Overnight capital costs of nuclear construction in major countries. Most countries report values exceeding $2000 kW^{-1} with the U.S. surpassing $4000 per kW[9,64,65]. **b** Comparison of nuclear levelized cost of electricity (LCOE) with other sources. In most countries, nuclear LCOE exceeds that of solar photovoltaic (PV) ($47 MWh^{-1}) and onshore wind ($40 MWh^{-1}). In the U.S., initial capital expenditures account for over 50% of the total LCOE, highlighting investment cost as a dominant driver[22,52]. **c** Changes in global nuclear capacity over the past 20 years, reported in five-year intervals (A, added; R, retired). While total installed capacity has slightly increased, most traditional nuclear countries show declining trends[1,66,67]. **d** Country-level nuclear capacity trends. Over the past two decades, nuclear additions have primarily occurred in China and other emerging markets, whereas traditional nuclear countries---led by the U.S.---have seen substantial retirements. Germany has fully phased out its nuclear fleet[1,66,67].

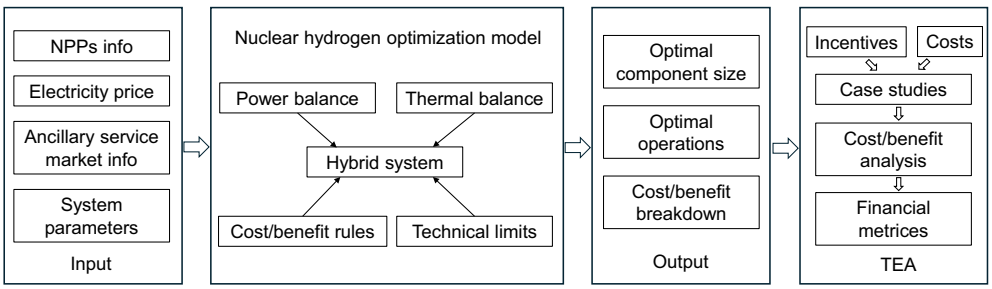


Fig. 2 | Modeling framework for the nuclear-hydrogen energy system optimization. The techno-economic analysis (TEA) framework consists of two main components. The first is an optimization model for the nuclear-hydrogen system, which incorporates system characteristics, electricity and ancillary service market data, and operational constraints to determine the optimal configuration and dispatch strategy. The second component uses the optimization outputs, policy incentives, and cost parameters to evaluate the system's techno-economic performance and compute key financial metrics, including net present value (NPV).

decreases the NPV by around $85 million for newly built nuclear-hydrogen systems. While the reduction in LCOH reflects improved capital cost amortization, the extended operational horizon increases cumulative long-term operation and maintenance (O&M) expenses, resulting in more negative NPVs under current cost structures (Fig. 3c).

Significant economic heterogeneity is observed across ISO regions, influenced by electricity price dynamics, ancillary service market design, and dispatch opportunities. ISO-NE and CAISO units achieve the highest average NPVs ($570 million and $360 million, respectively), while MISO and SPP units remain negative on average. PJM assets benefit from relatively high ancillary service revenues (nearly 4% of total income), whereas ERCOT units, despite high capacity factors, are constrained by low price volatility and limited surplus capacity. These regional disparities underscore the importance of location-specific modeling for evaluating retrofit potential (Fig. 3d).

Operational flexibility and ancillary services

To assess the flexibility enhancements enabled by system integration, a comprehensive analysis was conducted across all available ancillary services in the seven U.S. ISOs, considering each service's pricing structure, deployment frequency, and technical requirements. The modeling framework simulates bidding and deployment outcomes for Regulation Up/Down, Spinning/Non-Spinning Reserves, and Flex Ramp products where applicable. Reactor-specific technical constraints and operational limits of HTEs, including ramp rate limits, thermal inertia, and minimum stable load thresholds, are explicitly incorporated.

https://doi.org/10.1038/s41467-026-73630-y

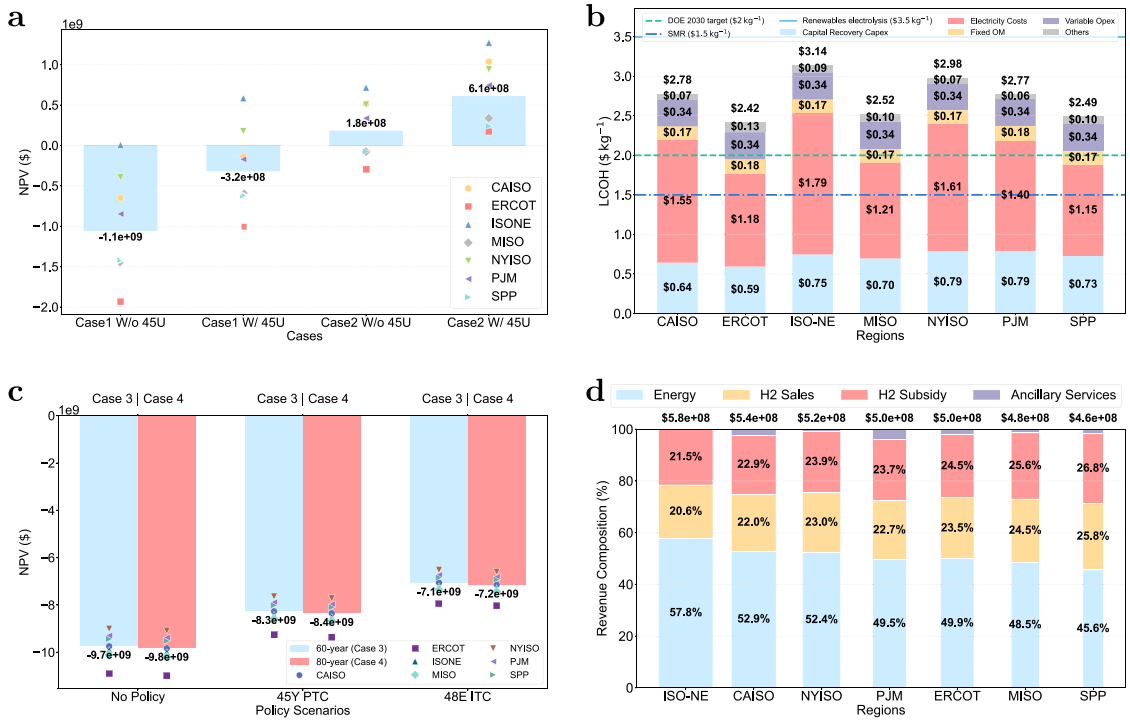


Fig. 3 | Economic performance of the nuclear-hydrogen system. a Net present value (NPV) of existing reactors under business-as-usual operation (Case 1) and retrofitted hybrid operation (Case 2), with and without the Section 45U production tax credit (45U PTC). Business-as-usual operation remains broadly unprofitable even with 45U support, whereas hybridization shifts the national average NPV to positive values and enables all reactors to achieve positive NPV when the 45U PTC is applied. **b** Levelized cost of hydrogen (LCOH) for hybrid systems across seven Independent System Operator (ISO) regions, benchmarked against the U.S. Department of Energy (DOE) 2030 target, steam methane reforming, and renewable-powered electrolysis. Regional LCOH values remain above the DOE target and steam methane reforming benchmark but below renewable-electrolysis costs, with electricity input and capital investment representing the dominant cost components. **c** NPV of newly built nuclear-hydrogen systems under 60- and 80-year lifespans and three policy scenarios: no credit, the Section 45Y production tax credit (45Y PTC), and the Section 48E investment tax credit (48E ITC). New-build systems remain NPV-negative under current cost assumptions, although policy incentives improve project economics. The 48E ITC provides the largest improvement, followed by the 45Y PTC. **d** Revenue composition of hybrid systems across seven ISO regions. Electricity sales provide the largest revenue stream, followed by hydrogen-related revenues from direct sales and the Section 45V hydrogen production tax credit (45V PTC). Ancillary service revenues contribute a smaller but additional value stream enabled by flexible hybrid operation.

The model also accounts for energy allocation trade-offs between electricity export, hydrogen production, and battery storage (where applicable). While some nuclear power plants in North America have demonstrated the capability to adjust output, such as daily load-following within a limited range, most have historically operated primarily as baseload generators, with minimal operational flexibility and no participation in ancillary service markets. Therefore, any observed increase in ramping capability, output variability, or ancillary service engagement within the integrated system represents a fundamental departure from conventional nuclear operation.

The integrated system exhibits a pronounced improvement in operational flexibility compared to conventional nuclear plants. Grid output variability, historically negligible for baseload units, becomes significantly more dynamic: the average coefficient of variation across all systems reached 2.14%, with a maximum of 4.16%. The dispatchable output range exceeded 115 MW for most systems, with a peak of 162.3 MW. This was further supported by an average maximum ramping capability exceeding 121 MW h^{-1} and peak ramp rates surpassing 162 MW h^{-1} for the most responsive units. On average, the integrated systems experienced over 500 ramping events annually, with some registering more than 950 events, highlighting a substantial increase in sub-hourly dispatch activity. Collectively, the systems delivered over 145,000 MWh of energy annually through ancillary service deployment, representing approximately 1.7% of total generation across all units. This contribution, rising from a baseline of zero ancillary service participation, underscores the transition of integrated systems toward a service-responsive generation paradigm (Fig. 4a).

Turbine-level flexibility was similarly enhanced. The turbine output range averaged 7.33 MW, with several units exceeding 9 MW. The turbine flexibility factor, a normalized measure of ramping potential, averaged 0.0065, reaching a peak of 0.0114. These metrics indicate a shift from static baseload operation toward active participation in intra-hour balancing. The number of turbine-associated ramping events ranged from 260 to over 950 per year, evidencing a marked increase in short-term dispatch responsiveness.

HTEs played a pivotal role in system-level flexibility by operating as stable yet responsive loads. With a capacity factor averaging 97.95% and continuous operation across all 8,760 hours, HTEs effectively absorbed excess generation while maintaining operational stability. Despite this constant operation, the average cycling frequency was below 0.07 per hour, reflecting minimal operational stress. A strong correlation between HTE cycling and high-frequency grid ramping activity was observed in 75% of units, suggesting dynamic coordination between generation variability and load absorption. In aggregate, HTEs consumed over 630,000 MWh of electricity annually, representing more than 7% of total system output. This substantial share highlights their role in improving flexibility, stabilizing operations, and creating headroom for ancillary service participation without compromising reliability. Together, turbines and HTEs form a tightly coupled flexibility backbone, enabling nuclear-hydrogen systems to meet

https://doi.org/10.1038/s41467-026-73630-y

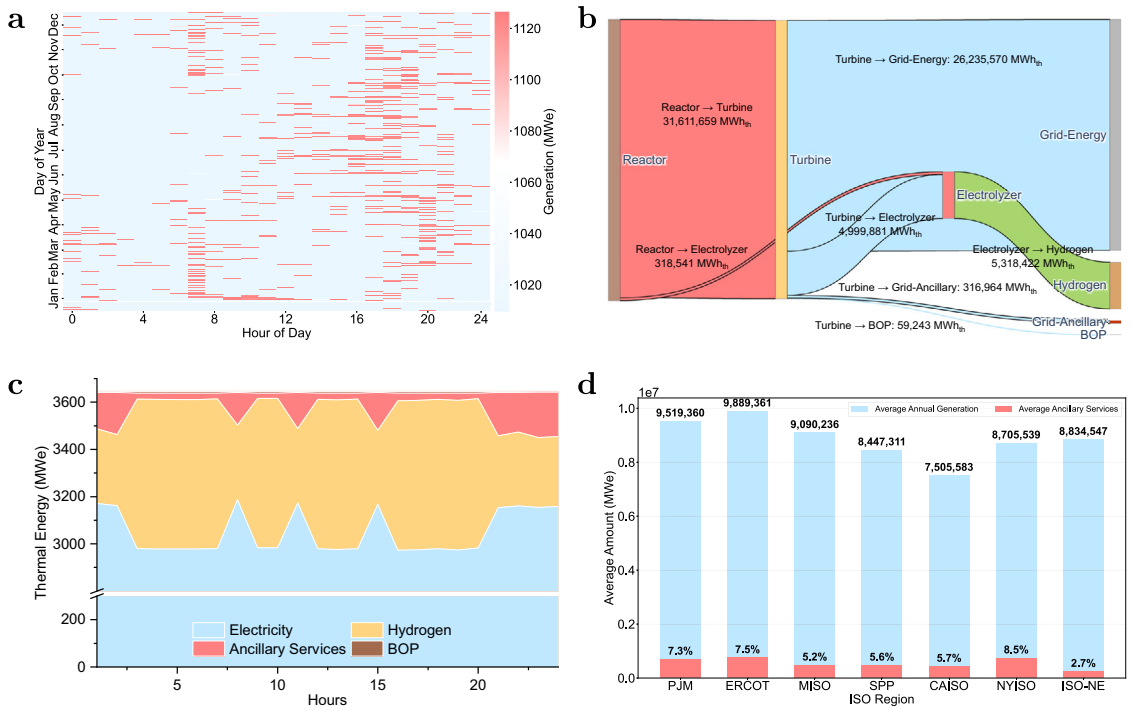


Fig. 4 | Operational flexibility of the nuclear-hydrogen system. a Hourly heatmap of electricity exported to the grid by a nuclear-hydrogen system in the PJM Interconnection (PJM) region over a full year. The system departs from a traditional baseload profile, exhibiting fluctuations exceeding 100 MW. Output closely follows grid demand, with near-maximum generation during morning and evening peaks and reduced output during off-peak hours, indicating strong load-following capability. **b** Annual energy flow within the system. Reactor thermal output remains constant, primarily powering the turbine, with a smaller portion directed to high-temperature electrolysis (HTE). In the secondary energy allocation, most turbine-generated electricity is exported to the grid, with the remainder used to power the HTE, supply ancillary services, and meet balance-of-plant (BOP) demand. **c** Hourly energy distribution breakdown. Consistent with the annual trend, most reactor energy is converted to electricity for export, followed by hydrogen production, ancillary services, and BOP, demonstrating efficient intra-system energy management. **d** Average share of reactor energy used for ancillary services across regions. Most regions maintain a 5–8% share, reflecting the system's active participation in ancillary markets. In contrast, ISO New England (ISO-NE) exhibits a lower share (2.7%) due to limited ancillary service offerings.

grid balancing demands previously inaccessible to standalone reactors (Fig. 4b, c).

The flexibility gains extend beyond technical improvements to generate economic value via participation in ancillary service markets. Simulation results indicate that all reactors successfully submitted offers for Regulation Up and Down services, with average offer sizes ranging from 20 to 40 MW per unit and offer variability exceeding 25% in over 60% of reactors. More than 80% of reactors achieved deployment frequencies above 0.3 for at least one ancillary service. In regions such as MISO, where RegDown products are available, deployment frequencies surpassed 0.6, significantly higher than median values in other regions. In ERCOT, some reactors secured over 3000 MWh of annual deployment through Non-Spinning Reserves. These patterns demonstrate that system flexibility interacts with ISO-specific service structures to create differentiated revenue streams. Therefore, the observed flexibility is both measurable and monetizable, with regionally dependent economic benefits (Fig. 4d).

Sensitivity analysis

We conducted three groups of sensitivity analyses to assess how key technical and economic parameters shape the performance of the nuclear–hydrogen integrated system. The first two analyses focus on a representative 1000 MW_{th} (380MW_e) nuclear facility operating within the ERCOT market framework. The first analysis explores the impact of nuclear fixed O&M costs on NPV and levelized cost of electricity (LCOE), while the second investigates how upper bounds on HTE capacity in the optimization model affect system operations and market performance. To further examine how broader market conditions may influence system economics, we introduce a third sensitivity analysis that evaluates alternative electricity price environments. Unlike the first two analyses, which focus on a representative reactor, this market-price sensitivity analysis is conducted across all reactors included in this study to capture regional market heterogeneity and maintain consistency with the reactor-level scope of the results presented earlier.

In the first analysis, we varied nuclear fixed O&M costs from \$170k MW^{-1} to \$290k MW^{-1}. Under the business-as-usual (BAU) (Case 1) scenario, even the lowest cost level fails to yield a positive NPV without tax credits, underscoring the inherent economic limitations of traditional nuclear systems. In contrast, the hybrid system shows strong economic sensitivity to this parameter. At \$170k MW^{-1}, NPV increases by over 130% compared to the baseline, reaching \$182 million. However, at \$290k MW^{-1}, NPV declines by more than 370%, turning negative. These results suggest that cost control of fixed O&M is critical for realizing economic gains from hybridization. Although the LCOE of the BAU system is less sensitive to this variable, a modest decrease is observed with lower O&M costs, as O&M accounts for only a small share of the LCOE while its effect on NPV accumulates over time (Fig. 5a).

In the second analysis, we examined the effect of varying the upper bound on HTE capacity in the optimization model, ranging from 100 MW to 300 MW. Although the model consistently selects the highest allowable value, the system response changes significantly. As the capacity limit increases, peak hourly hydrogen sales rise from 2217 kg h^{-1} to 4762 kg h^{-1}. When the limit is reduced below 200 MW, both the optimal hydrogen tank size and hydrogen sales volume decline. Increasing the limit beyond 200 MW leads to only marginal changes in tank size, but hourly hydrogen output remains high.

https://doi.org/10.1038/s41467-026-73630-y

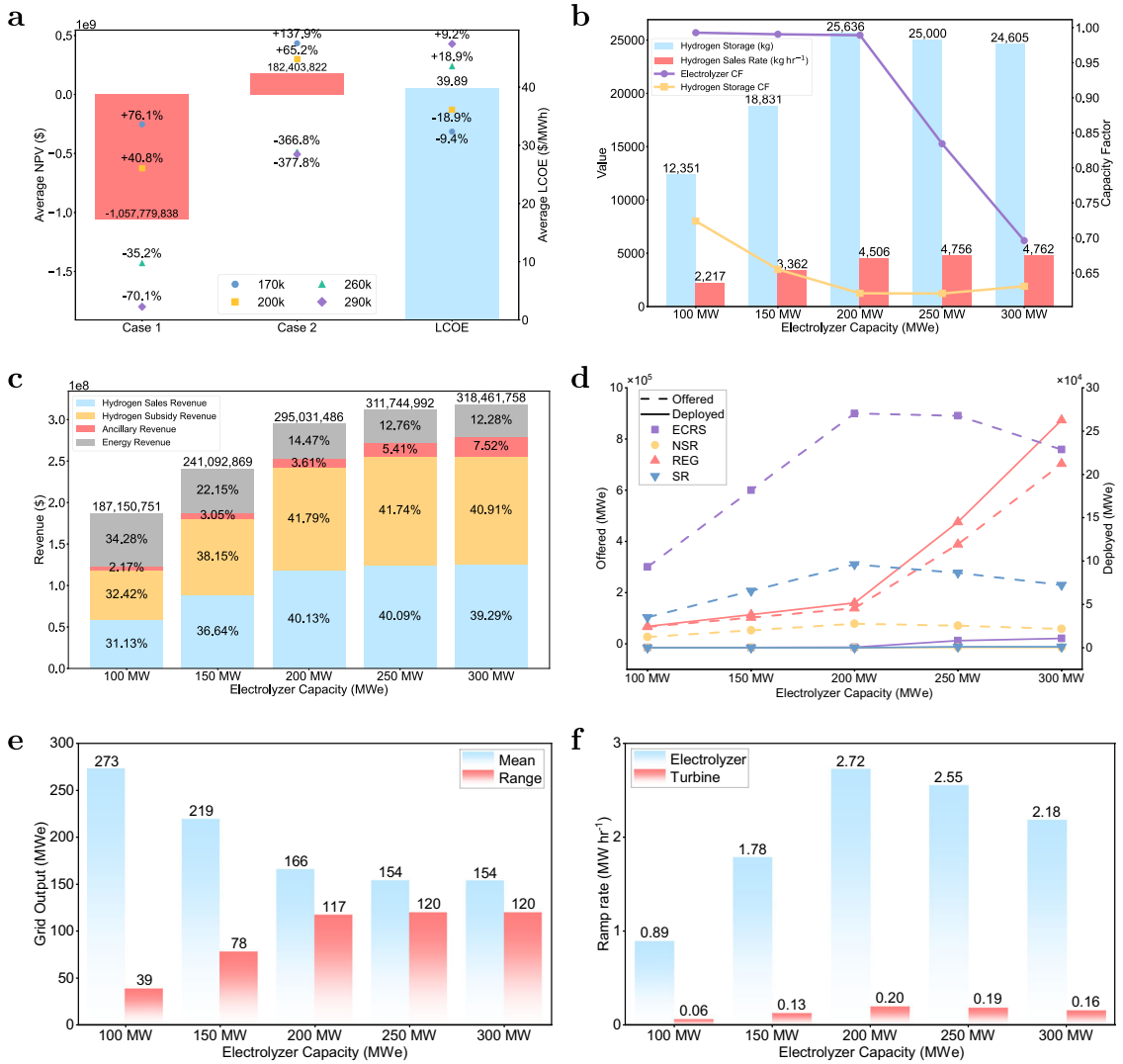


Fig. 5 | Sensitivity analysis of key system parameters. a Nuclear fixed operation and maintenance (O& M) cost sensitivity of net present value (NPV) under business-as-usual (BAU) and hybrid operation, showing that BAU remains unprofitable over the tested range, whereas hybrid-system profitability depends strongly on O& M cost control. **b** Effects of high-temperature electrolysis (HTE) capacity limits on hydrogen-system sizing and production, with lower limits reducing hydrogen storage capacity and hourly sales, while larger limits sustain higher production with reduced storage dependence. **c** Revenue response to HTE capacity limits, showing that larger HTE capacities increase total revenue and strengthen hydrogen and ancillary-service value streams, although hydrogen revenue declines slightly at the highest capacity because of reduced utilization. **d** Ancillary-service performance under different HTE capacity limits, showing that larger HTE capacities expand bidding capability and shift dispatch toward higher-value services such as regulation. **e** Grid power output range under different HTE capacity limits, showing that increased hydrogen production lowers average grid export but expands dispatchable output flexibility until constrained by total system energy availability. **f** Average ramp-rate response to HTE capacity limits, showing that flexibility increasingly shifts from the turbine to the HTE as capacity increases, with further ramping gains limited by system energy constraints.

Smaller HTE limits push the system to maximize storage utilization to sustain output. Conversely, larger HTE limits allow higher production rates that offset the need for extensive storage, even as utilization factors decline from 0.98 to 0.83 due to reactor energy constraints (Fig. 5b).

Total system revenue increases with higher HTE capacity limits, growing from $187 million at 100 MW to over $318 million at 300 MW. The share of hydrogen-related revenue also rises initially but drops slightly at 300 MW due to decreased utilization. In contrast, ancillary service revenue increases non-linearly, from 2.4% to 7.5% of total income, driven by enhanced system flexibility and market participation. This divergence reflects how HTE scaling not only affects energy production but also alters the balance of revenue sources, especially under flexibility-constrained scenarios (Fig. 5c).

As HTE capacity limits increase, the system bids more aggressively in ancillary service markets. Bid volumes grow across all service types, particularly for high-value regulation services. Beyond 200 MW, the bidding strategy prioritizes services with high deploy rates and economic returns, while maintaining reasonable bids for lower-value services. Even though bid volumes for some products decrease, actual deployment continues to rise, indicating that the system leverages its enhanced flexibility to pursue profit-optimized dispatch modes (Fig. 5d).

Net grid output declines from 273 MW to 154 MW as more energy is redirected to hydrogen production. However, the output range expands from 39 MW to 120 MW, with maximum flexibility achieved at the 250 MW limit. This behavior confirms that higher HTE capacities improve dispatchability, although further gains are limited by total system energy availability beyond this point (Fig. 5e).

HTE ramp rates rise with capacity, increasing from 0.89 MW h^{-1} to 2.18 MW h^{-1}. Turbine ramp rates also initially rise, but peak at 200 MW and then decrease from 0.20 MW h^{-1} to 0.16 MW h^{-1}. This shift

https://doi.org/10.1038/s41467-026-73630-y

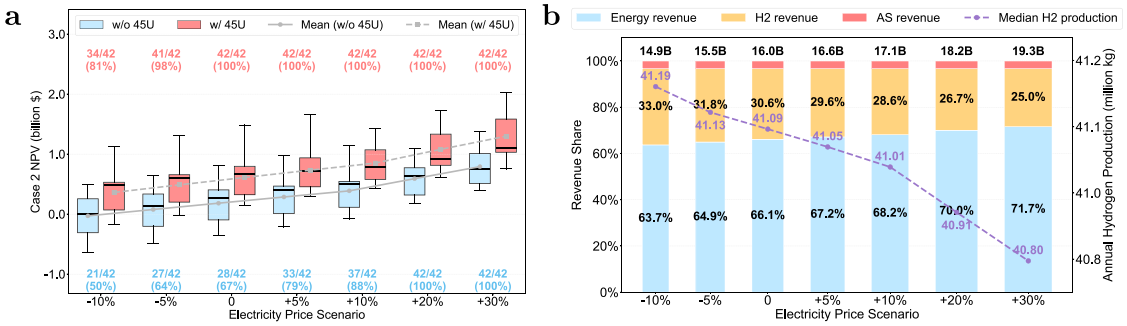


Fig. 6 | Electricity-price sensitivity of the nuclear-hydrogen system across all reactors. a Boxplots show the distribution of net present value (NPV) across all reactors for each electricity-price scaling scenario. Blue boxplots represent the no-45U case, and pink boxplots represent the case with the Section 45U production tax credit (45U PTC); solid gray lines indicate the mean NPV for the no-45U case, and dashed gray lines indicate the mean NPV for the 45U case. The annotations report the number and share of reactors with positive NPV in each scenario, illustrating how profitability thresholds shift with electricity-price levels and policy support. Center lines indicate medians, boxes indicate the interquartile ranges, and whiskers extend to 1.5 times the interquartile range. **b** Stacked bars show the revenue shares from electricity sales, hydrogen, and ancillary services under each electricity-price scenario, where bar width is proportional to total annual revenue (values annotated). As electricity prices increase, the system's value stream progressively shifts toward higher energy-market revenues, while hydrogen revenues decline and ancillary-service revenues remain relatively stable. The overlaid line reports the median annual hydrogen production across reactors, indicating that hydrogen output decreases as electricity prices rise, consistent with a reallocation of nuclear generation from electrolysis toward electricity sales.

indicates that flexibility responsibilities increasingly shift to the HTE, relieving mechanical stress on the turbine and allowing more dynamic system response. At high capacities, total system energy constraints cap further improvements in ramp performance (Fig. 5f).

For the electricity price sensitivity analysis, the 2024 electricity price profile used in the baseline model serves as the reference scenario. However, electricity prices may vary significantly over time due to changes in energy demand, fuel costs, and generation mix. Historical data from the U.S. Energy Information Administration (EIA) show that the national average electricity price increased by approximately 28% over the past five years[48], highlighting the potential for substantial price variation in future market environments. To capture this uncertainty, we construct six alternative price scenarios by adjusting the baseline electricity prices by − 10%, − 5%, + 5%, + 10%, + 20%, and + 30%. A greater number of upward scenarios are included to reflect the recent upward price trend and the possibility of increased electricity demand driven by factors such as the rapid expansion of data centers and broader electrification. At the same time, downward scenarios are also considered to represent potential price reductions associated with large-scale renewable deployment and expanded generation supply. This analysis allows us to systematically evaluate how variations in electricity prices may influence the economic viability of nuclear–hydrogen hybrid systems under different market environments, thereby capturing potential interannual variability in electricity prices and providing a broader representation of plausible future market conditions.

Across the electricity price scenarios, the retrofit hybrid configuration (Case 2) shows a monotonic improvement in profitability, while retaining substantial cross-reactor heterogeneity (Fig. 6a). Without 45U, the share of reactors with positive NPV increases from 21/42 (50%) at − 10% to 28/42 (67%) under the 2024 baseline, and reaches 42/42 (100%) at + 20% and + 30%. The mean NPV correspondingly shifts from − $29 million at − 10% to $182 million at the baseline and $791 million at + 30%. With 45U, profitability is more resilient under low-price conditions, rising from 34/42 (81%) positive-NPV reactors at − 10% to 42/42 (100%) from the baseline onward, and the mean NPV increases from $361 million at − 10% to $611 million at the baseline and $1.30 billion at + 30%.

Revenue decomposition indicates that rising electricity prices primarily increase total revenues through electricity sales, while the other value streams adjust more modestly (Fig. 6b). Total annual revenues increase from $14.9 billion at − 10% to $16.0 billion at the baseline and $19.3 billion at + 30%. Over this range, the energy revenue share increases from 63.7% to 71.7%, the hydrogen revenue share declines from 33.0% to 25.0%, and ancillary-service revenues remain relatively stable at around 3.3%. This pattern reflects an opportunity-cost mechanism: higher electricity prices raise the marginal value of selling power to the grid, reducing the incentive to allocate nuclear output to electrolysis and shifting value toward energy-market revenues. Consistent with this rebalancing, median annual hydrogen production decreases modestly from 41.19 to 40.80 million kilograms as electricity prices rise. The revenue and production responses illustrate how shifts in electricity price conditions propagate through the integrated configuration via opportunity costs, reshaping operating incentives and the relative contribution of each value stream, and thereby provide a transparent assessment of economic robustness across a broad range of plausible market environments.

Discussion

The U.S. nuclear fleet faces growing economic pressure in energy-only markets, where the inflexible nature of conventional baseload operation limits its ability to adapt to increasing renewable penetration and price volatility[49]. Our findings highlight that nuclear-hydrogen hybridization, specifically through HTE, offers a viable pathway to enhance both the operational flexibility and economic viability of these assets[50]. By enabling dynamic reallocation of thermal output among electricity generation, hydrogen production, and ancillary services, hybrid systems allow nuclear plants to respond to market signals and provide multi-vector energy services. This integrated configuration not only diversifies revenue streams but also repositions nuclear power as a flexible, low-carbon energy platform capable of supporting both grid reliability and clean fuel production.

Our analysis demonstrates that retrofitting existing reactors with HTE can substantially improve investment performance compared to the baseline case. The addition of hydrogen production reduces reliance on low wholesale power prices and captures emerging hydrogen market value, resulting in more favorable financial outcomes. While standalone hydrogen systems also show strong economic potential, particularly where low-cost electricity is available, integrated nuclear-hydrogen systems maximize synergies by using the stable, continuous thermal and electrical output of reactors. Federal incentives such as 45U, hydrogen production subsidy (45V), 45Y, and 48E play a critical role in narrowing cost gaps, but their effectiveness varies by

configuration and region, highlighting the importance of both technology improvements and supportive market mechanisms.

A key insight from this study is that flexibility is as important as cost reduction in achieving commercial viability. By enabling dynamic operation, integrated systems can participate in ancillary services, mitigate price volatility, and reduce curtailment, which collectively enhance total project value even if the LCOE rises due to additional investments. This value-stacking capability demonstrates that the profitability of hybrid nuclear-hydrogen projects is determined not by energy cost alone but by their ability to provide system-level services that are increasingly valuable in high-renewable grids.

Regional market characteristics strongly influence the achievable benefits of nuclear-hydrogen integration. Markets with robust ancillary service mechanisms and price variability offer greater opportunities for revenue diversification, while regions with suppressed power prices benefit from converting excess generation into clean hydrogen. These regional dynamics indicate that deployment strategies must be tailored to specific market conditions, and that regulatory frameworks should evolve to reward the flexibility and reliability that hybrid nuclear systems provide.

Sensitivity analysis underscores the importance of cost control and system design. Fixed operations and maintenance costs of nuclear reactors and the sizing of HTE capacity emerge as dominant drivers of project viability. Reducing O&M costs and optimizing electrolyzer sizing can significantly enhance returns, while misalignment between design choices and market conditions can erode value. In addition, the electricity price sensitivity analysis highlights that market price conditions can systematically reshape both profitability and operational incentives through opportunity-cost effects, shifting value between electricity sales and hydrogen production. These findings emphasize the need for integrated planning that considers both economic and technical factors when deploying hybrid systems, and for evaluating performance robustness across a range of plausible market environments rather than under a single historical price realization.

Looking forward, a phased deployment strategy is essential. Initial projects should focus on sites with favorable economic conditions, established hydrogen demand, and active ancillary service markets. Early deployments will provide critical operational experience, reduce perceived risk, and generate cost learning effects that can be leveraged in subsequent projects. Over time, scaling nuclear-hydrogen systems will contribute to lowering overall energy transition costs by offering a firm, flexible, and reliable energy supply, as well as producing affordable hydrogen for industrial and transportation sectors.

At the system level, hybrid nuclear-hydrogen plants can deliver multiple benefits beyond individual project economics. They can stabilize renewable-heavy grids, reduce reliance on fossil backup, and supply clean hydrogen for industry and transportation, effectively bridging the gap between the power and hydrogen sectors. These contributions are particularly valuable during the transition to a fully integrated energy system, where flexible, dispatchable, and carbon-free resources are critical.

Nevertheless, this study has limitations that should guide future research. Hydrogen price trajectories, regional demand profiles, and policy environments remain uncertain, and our modeling does not fully capture the potential impacts of future market evolution or broader sectoral integration (e.g., ammonia, synthetic fuels, or carbon capture). In particular, we treat electricity and hydrogen prices as exogenous inputs and do not explicitly model endogenous price formation and strategic feedback between coupled electricity–hydrogen markets. Recent studies have proposed equilibrium- and game-theoretic formulations (e.g., bi-level Stackelberg or market-clearing models) to capture these interdependencies and price-maker behavior[51]. Future work could integrate such coupled market representations with plant-level operational optimization to quantify how large-scale deployment of nuclear–hydrogen systems may influence market prices and, in turn, project economics. In addition, the present framework does not explicitly incorporate capacity market revenues or accreditation effects, which may represent an important component of nuclear plant economics in several U.S. ISO regions. Because capacity compensation depends on ISO-specific qualification, derating, deliverability, and forward market clearing rules rather than hourly dispatch alone, rigorously assessing the effect of nuclear–hydrogen integration on capacity payments would require a dedicated representation of regional capacity market mechanisms. Future work should therefore extend the current framework to evaluate how hydrogen integration may affect accredited capacity and capacity-market revenues under different ISO rules. Further engineering assessments and lifecycle analyses of HTE systems are needed to refine cost and performance assumptions.

Nuclear-hydrogen hybridization offers a compelling strategy to enhance the economic resilience and strategic role of nuclear power in a decarbonized future. Realizing this potential will require a combination of cost reduction, flexible operation, targeted incentives, and market designs that reward both low-carbon, reliable energy and grid services. By redefining nuclear power as a versatile energy hub rather than a static baseload source, this approach can strengthen the pathway to a more integrated energy system while unlocking new value streams for legacy and future nuclear assets.

Methods

Optimization model formulation

This section presents the mathematical formulation of the techno-economic optimization model for the Integrated Energy System (IES). The model is formulated as a Mixed-Integer Linear Program (MILP) to maximize the annual profit of the system by co-optimizing its participation in various energy and ancillary service markets. The core of the model consists of an objective function to be maximized, subject to a series of physical, operational, and economic constraints that govern the behavior of the system components. These components include an NPP, a water electrolyzer for hydrogen production, a battery energy storage system (BESS), and hydrogen storage.

Objective function. The objective of the model is to maximize the total profit (Π) over the optimization horizon. Profit is defined as total revenues minus total operational and annualized capital costs, as shown in equation (1).

$$\Pi = (R^{E} + R^{H_2} + R^{\mathrm{AS}}) - (C^{\mathrm{OPEX}} + C^{\mathrm{CAPEX}}) \tag{1}$$

Revenue components. Revenue from selling electricity to the grid minus the cost of purchasing electricity from the grid is defined in equation (2).

$$R^{E} = \sum_{t \in T} \Delta t \cdot \lambda_t^{E} \cdot (p_t^{sale} - p_t^{buy}) \tag{2}$$

Revenue from selling hydrogen, including any production subsidies, is defined in equation (3). This revenue is based on sales from storage, while subsidies are based on total production.

$$R^{H_2} = \sum_{t \in T} \Delta t \cdot \left((\dot{m}_t^{stor,out} + \dot{m}_t^{H_2,market}) \cdot \lambda^{H_2} + \dot{m}_t^{H_2} \cdot \lambda^{H_2,sub} \right) \tag{3}$$

Revenue from participating in ancillary service markets is defined in equation (4). This includes payments for capacity reservation and energy/performance payments upon deployment. The formulation varies by market. For a generic reserve service s:

$$R_s^{AS} = \sum_{t \in T} \Delta t \cdot \left(b_{t,s} \cdot w_{t,s} \cdot \lambda_{t,s}^{AS,cap} + \mathrm{EnergyPayment}_s \right) \tag{4}$$

where the energy payment for service s is given by $b_{t,s} \cdot w_{t,s} \cdot \delta_{t,s} \cdot \lambda_t^E$.

Cost components. The sum of all variable operational costs is defined by equation (5).

$$C^{OPEX} = \sum_{t\in T} \Delta t \cdot \left(C^{turb,vom} \cdot p_t^{turb} + C^{elec,vom} \cdot p_t^{elec} + C^{H_2O} \cdot \dot{m}_t^{H_2} + C^{b,vom} \cdot \frac{p_t^{b,ch} + p_t^{b,dis}}{2} + C^{stor,vom} \cdot (\dot{m}_t^{stor,in} + \dot{m}_t^{stor,out}) \right) + \sum_{t\in T} C^{elec,su} \cdot v_t^{elec} \quad (5)$$

The annualized capital cost of all dynamically sized components is scaled to the simulation period, as shown in equation (6).

$$C^{CAPEX} = \frac{|T| \cdot \Delta t}{8760} \left(C^{elec,capex} P_{max}^{elec} + C^{b,capex,E} E_{max}^{b} + C^{b,capex,P} P_{max}^{b} + C^{stor,capex} M_{max}^{stor} \right) \quad (6)$$

Constraints. System-level constraints. Power balance. The net power generated by the IES must equal the net power exchanged with the grid, as defined by equations (7) and (8).

$$p_t^{turb} + p_t^{b,dis} - p_t^{elec} - p_t^{b,ch} = p_t^{IES} \; \forall t \in T \quad (7)$$

$$p_t^{IES} = p_t^{sale} - p_t^{buy} \; \forall t \in T \quad (8)$$

Steam balance. The total steam produced by the reactor must be consumed by the turbine and the HTE, as shown in equation (9).

$$q_t^{turb} + q_t^{elec} = Q^{steam,total} \; \forall t \in T \quad (9)$$

Nuclear turbine constraints. Operating limits. Turbine power output is constrained by its operational limits, as shown in equation (10).

$$P_{min}^{turb} \le p_t^{turb} \le P_{max}^{turb} \; \forall t \in T \quad (10)$$

Ramp rates. The change in turbine power output between consecutive time periods is limited by equations (11) and (12).

$$p_t^{turb} - p_{t-1}^{turb} \le R_{max}^{turb,up} \cdot \Delta t \; \forall t \in T, t > 1 \quad (11)$$

$$p_{t-1}^{turb} - p_t^{turb} \le R_{max}^{turb,down} \cdot \Delta t \; \forall t \in T, t > 1 \quad (12)$$

Piecewise efficiency. Turbine power output (p_t^{turb}) is a piecewise linear function of its steam consumption (q_t^{turb}), as defined by equations (13)–(16).

$$q_t^{turb} = \sum_{k\in K_{turb}} \lambda_{t,k} \cdot Q_k^{turb,bp} \; \forall t \in T \quad (13)$$

$$p_t^{turb} = \sum_{k\in K_{turb}} \lambda_{t,k} \cdot P_k^{turb,bp} \; \forall t \in T \quad (14)$$

$$\sum_{k\in K_{turb}} \lambda_{t,k} = 1 \; \forall t \in T \quad (15)$$

$$\{\lambda_{t,k}\}_{k\in K_{turb}} \text{ isanSOS2set} \; \forall t \in T \quad (16)$$

Electrolyzer constraints. Operating limits. Electrolyzer power consumption is constrained by equations (17) and (18). If startup/shutdown logic is enabled, these limits are gated by the binary status variable u_t^{elec}.

$$p_t^{elec} \ge P_{min}^{elec,on} \cdot u_t^{elec} \; \forall t \in T \quad (17)$$

$$p_t^{elec} \le P_{max}^{elec} \cdot u_t^{elec} \; \forall t \in T \quad (18)$$

Ramp rates. The change in electrolyzer power consumption is limited by equations (19) and (20).

$$p_t^{elec} - p_{t-1}^{elec} \le P_{max}^{elec} \cdot R_{max}^{elec,up} \cdot \Delta t \; \forall t \in T, t > 1 \quad (19)$$

$$p_{t-1}^{elec} - p_t^{elec} \le P_{max}^{elec} \cdot R_{max}^{elec,down} \cdot \Delta t \; \forall t \in T, t > 1 \quad (20)$$

Piecewise efficiency (hydrogen production). Hydrogen production rate ($\dot{m}_t^{H_2}$) is a piecewise linear function of electrolyzer power consumption (p_t^{elec}), as defined by equations (21)–(24).

$$p_t^{elec} = \sum_{j\in K_{elec}} \lambda_{t,j} \cdot P_j^{elec,bp} \; \forall t \in T \quad (21)$$

$$\dot{m}_t^{H_2} = \sum_{j\in K_{elec}} \lambda_{t,j} \cdot \dot{M}_j^{H_2,bp} \; \forall t \in T \quad (22)$$

$$\sum_{j\in K_{elec}} \lambda_{t,j} = 1 \; \forall t \in T \quad (23)$$

$$\{\lambda_{t,j}\}_{j\in K_{elec}} \text{ isanSOS2set} \; \forall t \in T \quad (24)$$

A similar piecewise formulation is used to link steam consumption (q_t^{elec}) to power consumption (p_t^{elec}) for the HTE.

Startup/shutdown logic. These constraints manage the on/off state of the electrolyzer and enforce minimum uptime and downtime, as defined by equations (25)–(28).

$$u_t^{elec} - u_{t-1}^{elec} = v_t^{elec} - w_t^{elec} \; \forall t \in T, t > 1 \quad (25)$$

$$v_t^{elec} + w_t^{elec} \le 1 \; \forall t \in T \quad (26)$$

$$\sum_{i=t-T_{min}^{elec,up}+1}^{t} u_i^{elec} \ge T_{min}^{elec,up} \cdot v_t^{elec} \; \forall t \ge T_{min}^{elec,up} \quad (27)$$

$$\sum_{i=t-T_{min}^{elec,down}+1}^{t} (1 - u_i^{elec}) \ge T_{min}^{elec,down} \cdot w_t^{elec} \; \forall t \ge T_{min}^{elec,down} \quad (28)$$

Degradation tracking. The cumulative degradation of the electrolyzer is tracked by equation (29).

$$d_t = d_{t-1} + \left(D_{op} \cdot \frac{p_t^{elec}}{P_{max}^{elec}} \cdot \Delta t \right) + (D_{su} \cdot v_t^{elec}) \; \forall t \in T, t > 1 \quad (29)$$

Battery storage constraints. State-of-charge balance. The battery's state of charge is tracked over time, accounting for charge/discharge efficiencies, as shown in equation (30).

$$e_t^b = e_{t-1}^b + \Delta t \cdot \left(\eta^{b,ch} p_t^{b,ch} - \frac{p_t^{b,dis}}{\eta^{b,dis}} \right) \; \forall t \in T, t > 1 \quad (30)$$

Equation (30) is adjusted for $t = 1$ to use the initial state of charge E^b_{init}.

Operating and sizing limits. Battery operating and sizing limits are defined by equations (31)–(35).

$$p^{b,ch}_t \le P^b_{max} \cdot u^{b,ch}_t \; \forall t \in T \tag{31}$$

$$p^{b,dis}_t \le P^b_{max} \cdot u^{b,dis}_t \; \forall t \in T \tag{32}$$

$$u^{b,ch}_t + u^{b,dis}_t \le 1 \; \forall t \in T \tag{33}$$

$$E^b_{max} \cdot \mathrm{SOC}_{min} \le e^b_t \le E^b_{max} \; \forall t \in T \tag{34}$$

$$P^b_{max} = E^b_{max} \cdot \mathrm{PowerRatio}\,(\mathrm{If sizing}) \tag{35}$$

Hydrogen storage constraints. Storage balance. The mass of hydrogen in storage is tracked over time by equation (36).

$$m^{stor}_t = m^{stor}_{t-1} + \Delta t \cdot \left(\eta^{stor,ch} \dot{m}^{stor,in}_t - \frac{\dot{m}^{stor,out}_t}{\eta^{stor,dis}} \right) \forall t \in T, t > 1 \tag{36}$$

Production and sales dispatch. Hydrogen produced can be sent to storage or directly to the market, as required by equation (37).

$$\dot{m}^{H_2}_t = \dot{m}^{H_2,market}_t + \dot{m}^{stor,in}_t \; \forall t \in T \tag{37}$$

Operating and sizing limits. Hydrogen storage operating and sizing limits are given by equations (38)–(40).

$$M^{stor}_{min} \le m^{stor}_t \le M^{stor}_{max} \; \forall t \in T \tag{38}$$

$$\dot{m}^{stor,in}_t \le \dot{M}^{stor,ch}_{max} \; \forall t \in T \tag{39}$$

$$\dot{m}^{stor,out}_t \le \dot{M}^{stor,dis}_{max} \; \forall t \in T \tag{40}$$

When optimal H_2 storage sizing is enabled, a constant hydrogen sales rate is enforced ($\dot{m}^{stor,out}_t = \dot{m}^{H_2,sale}_{const}$), and all hydrogen production is routed through storage ($\dot{m}^{H_2,market}_t = 0$).

Ancillary service constraints. Component capability. The bids for ancillary services from each component are limited by the component's physical headroom and ramp rates. For upward reserve from the turbine, the limit is given by equation (41).

$$p^{turb}_t + \sum_{s \in S_{up}} b^{turb}_{t,s} \le P^{turb}_{max} \; \forall t \in T \tag{41}$$

For downward reserve from the electrolyzer (load increase), the limit is given by equation (42).

$$p^{elec,sp}_t + \sum_{s \in S_{down}} b^{elec}_{t,s} \le P^{elec}_{max} \cdot u^{elec}_t \; \forall t \in T \tag{42}$$

Similar constraints exist for all services on all components, including ramp rates and battery state of charge.

Bid aggregation. The total bid for each service is the sum of bids from all participating components, as shown in equation (43).

$$b_{t,s} = \sum_{c \in C} b^c_{t,s} \; \forall t \in T, s \in S \tag{43}$$

Regulation balance. For certain markets, regulation up and down bids must be equal for each component, as defined by equation (44).

$$b^c_{t,\mathrm{RegUp}} = b^c_{t,\mathrm{RegDown}} \; \forall t \in T, c \in C \tag{44}$$

Dispatch execution mode constraints. Deployed amount. In this mode, the deployed amount of an ancillary service is linked to the winning bid, as shown in equation (45).

$$d^c_{t,s} = b^c_{t,s} \cdot w_{t,s} \cdot \delta_{t,s} \; \forall t \in T, s \in S, c \in C \tag{45}$$

Actual power adjustment. The actual power of a component is adjusted based on its setpoint and the amount of ancillary service it deploys. For the electrolyzer, this relationship is given by equation (46).

$$p^{elec}_t = p^{elec,sp}_t - \sum_{s \in S_{up}} d^{elec}_{t,s} + \sum_{s \in S_{down}} d^{elec}_{t,s} \; \forall t \in T \tag{46}$$

Techno-economic analysis framework

This section details the methodology of the TEA framework developed to evaluate the financial viability of nuclear-hydrogen IESs. The framework is designed to be comprehensive, incorporating detailed cost models, operational simulations, and the impact of federal tax incentives. It analyzes various scenarios, from retrofitting existing NPPs to developing new greenfield projects with different operational lifetimes. The core of the framework is a discounted cash flow (DCF) analysis, which is used to calculate key financial performance indicators.

Core financial principles and metrics. The primary financial evaluation is based on a DCF analysis over the project's entire lifecycle, from construction to decommissioning. The fundamental metric is the NPV, which represents the total value of the project in today's currency. The NPV is calculated as the sum of all discounted future cash flows, as shown in equation (47).

$$\mathrm{NPV} = \sum_{t=0}^{N} \frac{\mathrm{CF}_t}{(1+r)^t} \tag{47}$$

where CF_t is the net cash flow in year t, r is the discount rate, and N is the total project lifetime in years.

The annual net cash flow (CF_t) for each operational year is determined by accounting for all revenues, operating expenditures (OPEX), and the tax implications of depreciation. The after-tax cash flow is calculated using equation (48).

$$\mathrm{CF}_t = (R_t - C_{\mathrm{OPEX},t} - D_t)(1-\tau) + D_t \tag{48}$$

where R_t is the total annual revenue, $C_{\mathrm{OPEX},t}$ is the total annual operating expenditure, D_t is the annual depreciation allowance, and τ is the corporate tax rate. The term $D_t \cdot \tau$ represents the tax shield provided by depreciation, which is a non-cash expense that reduces the project's tax burden.

Other key financial indicators derived from the cash flow analysis include the internal rate of return (IRR), which is the discount rate at which the NPV of the project becomes zero, and a project is considered financially attractive if its IRR exceeds the minimum acceptable rate of return or the cost of capital; the payback period, which is the time required for the cumulative cash flows from a project to equal the initial investment, thereby providing insight into the project's risk and liquidity; and levelized costs, which are the average net present cost of a technology per unit of output over its lifetime. The framework

calculates the LCOH, LCOE, and levelized cost of storage (LCOS) using a detailed, independent accounting methodology, as described in a later section.

Capital expenditure modeling. The framework employs a detailed, component-based model for capital expenditures. The total capital expenditure (CAPEX) is disaggregated into major systems, including the nuclear island, turbine generator, hydrogen production system (electrolyzer, storage), and battery storage system. For greenfield projects, this also includes site preparation and grid connection costs. This granular approach allows for the application of technology-specific cost-scaling and learning rates. The cost of a component is scaled from a reference size using a learning rate to account for economies of scale, as calculated by equation (49).

$$C_{adj} = C_{ref}\left(\frac{S_{actual}}{S_{ref}}\right)^{\alpha} \tag{49}$$

where C_{adj} is the adjusted cost for the component, C_{ref} is the base cost for a reference size S_{ref}, S_{actual} is the actual capacity of the component, and α is the scaling exponent, derived from a specified learning rate. Capital investments are distributed over the construction period according to predefined payment schedules for each major component.

Major component replacements are modeled as capital outflows in the specific years they are scheduled to occur. The framework uses a detailed replacement schedule, for instance[52]: electrolyzer stacks are replaced every 10 years, battery systems are replaced every 10 years, and major hydrogen storage components are replaced every 15 years.

Operating expenditure modeling. Annual operating costs are modeled with a similar level of detail. Operating expenditure (OPEX) is separated into fixed and variable components. Fixed OPEX includes costs that do not vary with production, such as salaries, insurance, and routine maintenance. These are calculated on a per-megawatt-year basis, for example, $\$\,MW^{-1}\,year^{-1}$, and are subject to an annual inflation rate. Variable OPEX (VOM) includes costs directly tied to system operation, such as consumables, water for electrolysis, and component wear. These are calculated on a per-megawatt-hour basis, for example $\$\,MWh^{-1}$, or on a per-kilogram basis, for example $\$\,kg^{-1}$. Nuclear fuel costs, as a major component of nuclear OPEX, are calculated on a per-megawatt-hour basis of electricity generation in the baseline case, whereas in the retrofitted hybrid system, they are calculated based on the actual energy output of the reactor.

Revenue and opportunity cost modeling. The framework considers multiple revenue streams, including electricity sales to the grid, hydrogen sales, and ancillary services, with a particular emphasis on modeling opportunity costs. When the nuclear plant diverts electricity or heat to hydrogen production, it forgoes potential revenue from electricity sales to the grid, which is explicitly treated as an opportunity cost in assessing hydrogen production profitability. Similarly, providing ancillary services may require the plant or electrolyzer to operate at suboptimal levels for energy sales, and the resulting opportunity cost is also accounted for. In the case of HTE, the diversion of steam from the turbine reduces potential electricity generation, and the corresponding opportunity cost is quantified based on the plant's thermal efficiency and prevailing electricity prices.

Depreciation and taxation. The framework implements the Modified Accelerated Cost Recovery System (MACRS) for asset depreciation, which provides a significant tax shield[53]. Assets are classified into different schedules based on their type, reflecting U.S. tax law. A 15-year MACRS schedule is applied to NPP equipment and grid infrastructure, whereas a 7-year MACRS schedule is applied to hydrogen production and battery storage equipment. The annual depreciation for each class is calculated according to the schedules provided in Table 1. The total depreciation allowance in any given year is the sum of the depreciation from all assets, which is then used to calculate the project's tax liability.

Table 1 | Modified accelerated cost recovery system (MACRS) depreciation schedules

7-Year Property		15-Year Property	
Year	Rate (%)	Year	Rate (%)
1	14.29	1	5.00
2	24.49	2	9.50
3	17.49	3	8.55
4	12.49	4	7.70
5	8.93	5	6.93
6	8.92	6	6.23
7	8.93	7–15	5.90
8	4.46	16	2.95

Federal tax incentive analysis. An important feature of the framework is its capability to simulate the effects of several major U.S. federal tax incentives. In this study, particularly for hybrid systems combining nuclear power and hydrogen production, we assume that the system can simultaneously benefit from both hydrogen-related and nuclear-related incentive schemes, with each calculated according to its respective methodology and then aggregated.

The 45U PTC is specifically for existing NPPs. For electricity generated between 2024 and 2032, the credit amount is determined dynamically based on the hourly electricity market price, decreasing linearly as the price increases from $\$25\,MWh^{-1}$ to $\$43.75\,MWh^{-1}$. The hourly credit value (C_{45U}) is computed as a function of the market price (P_{market}) using equation (50). In this study, a streamlined implementation of the 45U credit adjustment is used to reflect the policy's essential price-responsive structure in a form suitable for integrated system modeling[16].

$$C_{45U}(P_{market}) = \begin{cases} \$15 & \text{if } P_{market} < \$25.0 \\ \$15 \times \left(1 - \frac{P_{market} - \$25.0}{\$18.75}\right) & \text{if } \$25.0 \le P_{market} \le \$43.75 \\ \$0 & \text{if } P_{market} > \$43.75 \end{cases} \tag{50}$$

The 45Y clean electricity PTC is for new zero-emission power facilities, including new nuclear plants. The framework models this as a credit of up to $\$30\,MWh^{-1}$ for the first 10 years of the plant's operation. This credit is a direct addition to the project's annual cash flow[54].

The 48E clean electricity ITC is an alternative to the 45Y PTC for new facilities. The ITC provides an upfront tax credit based on the initial capital investment. The model implements a credit of up to 50% on qualified capital expenditures. Crucially, the model correctly applies this credit only to the nuclear power generation equipment, excluding hydrogen and battery assets. Furthermore, it implements the required depreciation basis reduction, where the asset's value for depreciation purposes is reduced by 50% of the claimed ITC value, as defined by equation (51)[54].

$$\text{DepreciableBasis}_{adj} = \text{CAPEX}_{original} - 0.5 \times \text{ITC}_{value} \tag{51}$$

This reduction lowers the total depreciation tax shield over the asset's life, partially offsetting the benefit of the upfront credit.

The framework also includes a generic hydrogen production subsidy, modeled after policies like 45V, which provides a direct payment of up to $\$3.00\,kg^{-1}$ of clean hydrogen produced for verified use during the first 10 years of operation. In this study, we assume the maximum rate of $\$3.00\,kg^{-1}$ applies uniformly across all scenarios[55].

Case study design. The TEA framework is applied across four distinct case studies to provide a holistic view of the economic potential of nuclear-hydrogen systems.

Case 1: Existing reactor baseline. This case serves as the financial benchmark. It analyzes the business-as-usual operation of an existing NPP without any modifications for hydrogen production. The analysis uses the plant's actual remaining operational lifetime and calculates revenue based on selling all generated electricity to the grid at hourly market prices. The key objective is to determine the standalone profitability of the existing asset and to analyze the potential financial uplift from the 45U PTC.

Case 2: Existing reactor retrofit. This case evaluates the economic viability of retrofitting an existing NPP with an integrated hydrogen production and battery storage system. The analysis includes the CAPEX for the new hydrogen and battery assets, but assumes the nuclear plant itself is a sunk cost. It calculates the combined revenue streams from electricity sales, hydrogen sales, and ancillary services. This case also considers the impact of the 45U PTC on the nuclear portion of the integrated system's revenue.

Case 3: Greenfield system (60-year lifecycle). This case examines a newly constructed, fully integrated nuclear-hydrogen-battery system with a 60-year operational lifetime. It includes the complete capital investment for the nuclear reactor and all non-nuclear subsystems. Three distinct policy scenarios are evaluated: (1) no federal incentives, (2) the 45Y PTC, and (3) the 48E ITC. This case evaluates the economics of greenfield nuclear-hydrogen systems over a standard design lifespan, considering current U.S. tax incentives and system cost structure.

Case 4: Greenfield system (80-year lifecycle). Building upon Case 3, this case extends the system's operational lifetime to 80 years to reflect the enhanced durability and lifespan potential of next-generation advanced reactors. The same three policy scenarios, namely no incentives, 45Y PTC, and 48E ITC, are analyzed to evaluate how extended operation alters the cost-effectiveness and policy impacts. This longer-term perspective captures additional revenue potential, offset by the need for more frequent equipment replacements and increased long-term maintenance costs, offering deeper insight into lifecycle financial dynamics.

Levelized cost calculation methodology. To provide a clear and fair comparison of costs, the framework utilizes an independent accounting methodology for calculating levelized costs. This approach avoids cross-subsidization between different parts of the integrated system.

Levelized cost of electricity. The LCOE represents the cost of generating electricity from the nuclear plant only. It is calculated by considering only the costs and revenues directly attributable to the nuclear power island and turbine generator, as shown in equation (52).

$$\mathrm{LCOE} = \frac{\mathrm{PV}(\mathrm{NuclearCAPEX} + \mathrm{NuclearOPEX} - \mathrm{TurbineASRevenue})}{\mathrm{PV}(\mathrm{TotalElectricityGeneration})} \tag{52}$$

Levelized cost of hydrogen. The LCOH is calculated for the hydrogen production system. Critically, the cost of electricity consumed by the electrolyzer is not assumed to be zero. It is valued at the LCOE calculated for the nuclear plant, representing a fair internal transfer price, as shown in equation (53).

$$\mathrm{LCOH} = \frac{\mathrm{PV}\left(\begin{array}{c}\mathrm{CAPEX}_{\mathrm{H_2}} + \mathrm{OPEX}_{\mathrm{H_2}} + \mathrm{Elec.Cost}_{\mathrm{LCOE}} \\ + \mathrm{HTECost} - \mathrm{ASRevenue}_{\mathrm{H_2}}\end{array}\right)}{\mathrm{PV}(\mathrm{Total H_2\ Production})} \tag{53}$$

Levelized cost of storage. Similarly, the LCOS for the battery system is calculated based on its own CAPEX, OPEX, and dedicated revenue streams, providing a clear picture of the cost per megawatt-hour of energy discharged from the battery over its lifetime, as shown in equation (54).

$$\mathrm{LCOS} = \frac{\mathrm{PV}(\mathrm{BatteryCAPEX} + \mathrm{BatteryOPEX} - \mathrm{BatteryASRevenue})}{\mathrm{PV}(\mathrm{TotalEnergyDischarged})} \tag{54}$$

Data generation and collection

To facilitate the testing and validation of our nuclear-hydrogen production optimization model, a comprehensive synthetic dataset was generated. This process, implemented in Python, creates internally consistent time-series data and system parameters that mimic real-world operational conditions. The generation process is deterministic, using a fixed random seed (`np.random.seed(42)`) to ensure the replicability of the entire dataset. The generated data encompasses techno-economic system parameters, hourly electricity prices, and detailed ancillary service market data for various ISOs.

System parameter formulation

A foundational set of techno-economic parameters is generated to define the physical and economic characteristics of the IES. These parameters are technology-specific and crucial for the optimization model's constraints and objective function.

Common and plant-wide parameters. To support system-level sensitivity analysis, a representative nuclear-hydrogen configuration was established using stylized core plant parameters: a 1000 MW_{th} thermal reactor coupled with a 380 MW steam turbine. This configuration defines the upper bounds for turbine power output ($P_{\mathrm{turbine}}^{\max} = 380.0$ MW) and total available thermal steam ($Q_{\mathrm{steam}}^{\mathrm{total}} = 1000.0$ MW_{th}), and assumes a 30-year project lifetime with a discount rate of r = 0.06. The turbine's operational range is characterized by minimum and maximum power and steam input limits, a piecewise linear thermal-electric efficiency curve based on steam flow breakpoints, and ramp rate constraints[9,50].

However, for the core optimization and TEA performed across 42 actual nuclear power plants, all nuclear-related system parameters, such as reactor thermal capacity, turbine power ratings, and conversion efficiency, are based on real plant-specific data. These technical specifications were obtained directly from the U.S. Nuclear Regulatory Commission (NRC) database, ensuring that the modeled system configurations reflect the actual physical and operational characteristics of each reactor[38].

Electrolyzer technology parameters. The model incorporates an HTE, representative of Solid Oxide Electrolysis Cell (SOEC) technology. A detailed set of techno-economic parameters is specified for this technology.

Capital cost. The annualized capital expenditure (CAPEX) is a critical cost component. It is derived from the overnight cost, the economic lifetime, and the discount rate using the Capital Recovery Factor (CRF). The CRF is calculated using equation (55).

$$\mathrm{CRF} = \frac{r(1+r)^L}{(1+r)^L - 1} \tag{55}$$

where r is the discount rate and L is the lifetime in years.

Efficiency and consumption. Electrolyzer efficiency is modeled as a piecewise linear function dependent on the electrical load. Four operating breakpoints are defined, starting from a minimum load of 10% of the maximum capacity (200 MW). Electrical consumption (k_e) for HTE ranges from 44.0 to 41.0 kWh kg^{-1}, reflecting its higher efficiency at operating temperatures. These values are converted to MWh kg^{-1} for the model[56]. Thermal consumption (k_t) for HTE requires thermal energy input, which is modeled as a constant 0.008 MWh_{th} kg^{-1} of hydrogen produced across all operating points[56].

Other operational parameters include variable O&M costs (6.9 $ MWh^{-1} for HTE), startup costs, ramp rates (expressed as a percentage of maximum capacity per minute), and minimum up/down times. Degradation is also modeled using distinct factors for steady-state operation and for each startup event[56].

Battery Energy Storage System parameters. A BESS is included as an optional system component. Its parameters are derived to reflect current technology costs and performance. Capital cost assumptions for the BESS are defined for both power and energy capacity. A total energy capital cost of $2.1M MW^{-1} and a 4-hour duration are assumed. The annualized power capacity cost is calculated using a 20-year lifetime and the CRF. The model is specifically configured to only consider the power capacity cost, setting the energy capacity cost to zero to analyze scenarios where power is the primary cost driver[52]. O&M cost is derived as a fraction of the power CAPEX (2.5%). Performance metrics include charge/discharge efficiency (both 92%), a minimum state of charge of 10%, and a power-to-energy ratio (P/E) of 0.25, corresponding to the 4-hour duration[52].

Time-series data generation and collection

Hourly data for a full year (8760 h) is generated to simulate market conditions. This includes ancillary services and operational factors. All electricity price inputs used in the model are based on the average 2024 locational marginal prices (LMPs) at the hub or node level, published by each ISO at 15 min resolution and aggregated to hourly values. Ancillary service price data were similarly obtained from each ISO's 2024 hourly publications. February 29th was excluded to ensure consistency with a 365-day calendar year, and missing values were linearly interpolated to obtain a complete dataset of 8760 hourly entries[39–45].

Ancillary service (AS) market data.

AS capacity prices. The market-clearing price for each ancillary service is generated based on the hourly LMP, assuming that AS prices are correlated with energy prices. The price is calculated using equation (56).

$$\text{Price}_{\text{AS}} = \max(0, \text{LMP} \times U(0.05, 0.4) + N(0, 3) + \text{Spike}) \quad (56)$$

where U is a uniform distribution, N is a normal distribution for noise, and Spike represents a 2% hourly probability of a price adder between $10 and $50. This creates AS prices that are fundamentally linked to energy scarcity but have their own distinct volatility.

Deployment, mileage and performance factors.

Due to the lack of publicly available high-resolution deployment records for ancillary services, all deployment-related inputs in this study were generated synthetically through a simulation-based framework. The generation process was informed by publicly available ISO documents, historical system operation data, and operational heuristics reported in prior literature[57–62].

For regulation services (e.g., RegUp/RegDown), where deployment frequency and directionality are critical but rarely disclosed, a paired simulation strategy was adopted. Hourly deployment probabilities were constructed using smoothed stochastic time series, incorporating both intra-day (three cycles per day) and weekly seasonalities. These patterns were calibrated to yield an average directional deployment bias of 0.44 in favor of regulation-up, consistent with empirical expectations of net upward control effort. To ensure system feasibility, the combined hourly deployment activity for regulation-up and regulation-down was constrained below 0.98, and post-processing adjustments were made to preserve both the directional bias and total activation limits.

For non-regulation reserve services (e.g., spinning, non-spinning, supplemental, and ramping reserves), deployment factors were similarly generated using category-specific probability and magnitude ranges. These ranges were derived from ISO-published simulation assumptions, such as those used in planning reserve margin studies or operational flexibility assessments. For each service, hourly deployment was determined by sampling a Bernoulli process governed by its probability envelope, with activated magnitudes drawn from uniform distributions within the category-specific operational band. This framework enables the representation of diverse service behaviors while maintaining cross-ISO consistency and interpretability.

Mileage multipliers and performance factors, essential for modeling the operational burden of regulation services, were likewise generated synthetically due to the unavailability of full-year, service-level data from ISOs. All parameterization was based on public ISO reports, simulation templates, and historical estimates.

For each ISO, regulation-up and regulation-down services were jointly modeled using base mileage values extracted from ISO-published simulation data (e.g., PJM's RegD mileage of 5.4, CAISO's 12.5, etc.). To reflect temporal variability and measurement uncertainty, independent Gaussian noise (scaled to 5–10% of the base mileage) was applied, and resulting values were clipped to maintain operational realism. Paired services within the same ISO (e.g., RegUp/RegDown) were assigned consistent mileage profiles to reflect the shared system control dynamics.

Performance factors were generated from a normal distribution centered at 0.95, with truncation at 0.7 and 1.0, reflecting the high but variable fidelity observed in actual Automatic Generation Control (AGC) regulation. Identical hourly performance factors were used for regulation-up and -down in each ISO to capture their joint dependence on telemetry precision, AGC latency, and plant control capabilities.

Data availability

The data supporting the findings of this study are publicly available in the GitHub repository Henryutd2021/NPPH2 and are permanently archived on Zenodo under the following https://doi.org/10.5281/zenodo.19646104[63].

Code availability

The code supporting the findings of this study is publicly available in the GitHub repository Henryutd2021/NPPH2 and are permanently archived on Zenodo under the following https://doi.org/10.5281/zenodo.19646104[63].

References

1. Fell, H., Gilbert, A., Jenkins, J. D. & Mildenberger, M. Nuclear power and renewable energy are both associated with national decarbonization. *Nat. Energy* **7**, 25–29 (2022).
2. Sovacool, B. K., Schmid, P., Stirling, A., Walter, G. & MacKerron, G. Differences in carbon emissions reduction between countries pursuing renewable electricity versus nuclear power. *Nat. Energy* **5**, 928–935 (2020).
3. Duan, L., Petroski, R., Wood, L. & Caldeira, K. Stylized least-cost analysis of flexible nuclear power in deeply decarbonized electricity systems considering wind and solar resources worldwide. *Nat. Energy* **7**, 260–269 (2022).
4. Greene, S. R. Are current us nuclear power plants grid resilience assets? *Nucl. Technol.* **202**, 1–14 (2018).
5. Chen, X., Huang, L., Liu, J., Song, D. & Yang, S. Peak shaving benefit assessment considering the joint operation of nuclear and battery energy storage power stations: Hainan case study. *Energy* **239**, 121897 (2022).
6. Price, J., Keppo, I. & Dodds, P. E. The role of new nuclear power in the uk's net-zero emissions energy system. *Energy* **262**, 125450 (2023).
7. Pehl, M. et al. Understanding future emissions from low-carbon power systems by integration of life-cycle assessment and integrated energy modelling. *Nat. Energy* **2**, 939–945 (2017).
8. Verbruggen, A. Renewable and nuclear power: A common future? *Energy Policy* **36**, 4036–4047 (2008).

9. Knighton, L. T. et al. Techno-economic analysis of product diversification options for sustainability of the monticello and prairie island nuclear power plants. Tech. Rep., Idaho National Lab.(INL), Idaho Falls, ID (United States) (2021).
10. Association, W. N. Economics of nuclear power.https://world-nuclear.org/ (2025).
11. ifp. What does it cost to build nuclear power.https://ifp.org/nuclear-power-plant-construction-costs/ (2025).
12. Root, S. J., Shigrekar, A. & Westover, T. L. Techno-economic analysis of a nuclear reactor system coupled with a liquid metal battery. *Tech. Rep.* https://doi.org/10.13182/T129-42651 (2023).
13. U.S. Energy Information Administration. We expect rapid electricity demand growth in texas and the mid-atlantic. https://www.eia.gov/todayinenergy/detail.php?id=65844 (2025).
14. PJM Interconnection, L.L.C. 2025 pjm long-term load forecast report. *Tech. Rep.*https://www.pjm.com/-/media/DotCom/library/reports-notices/load-forecast/2025-load-report.pdf (2025).
15. Constellation Energy Corporation. Constellation reports second quarter 2025 resultshttps://www.constellationenergy.com/newsroom/2025/08/constellation-reports-second-quarter-2025-results.html (2025).
16. Internal Revenue Service. Zero-Emission Nuclear Power Production Credithttps://www.irs.gov/credits-deductions/zero-emission-nuclear-power-production-credit (2023).
17. Idaho National Laboratory. Technical economic assessment of LWR-supported hydrogen markets in gulf coast regions. *Tech. Rep.*https://lwrs.inl.gov/flexible-plant-operation-and-generation-reports/ (2023).
18. Smola, T. et al. Integrated thermohydraulic transient testing of steam extraction loop system to support joint electricity-hydrogen production using generic boiling water reactor. *Prog. Nucl. Energy* **160**, 104692 (2023).
19. Mahmud, S. et al. Design and optimization of a modular hydrogen-based integrated energy system to maximize revenue via nuclear-renewable sources. *Energy* **313**, 133763 (2024).
20. Wendt, D., Neupane, G., Simpson, J. G., McTigue, J. & Zhu, G. Techno-economic analysis of greenfield geothermal hybrid power plants using a solar or natural gas steam topping cycle. *Tech. Rep.* https://www.inl.gov/ (2024).
21. Jain, R., Nagasawa, K., Veda, S. & Sprik, S. Grid ancillary services using electrolyzer-based power-to-gas systems with increasing renewable penetration. *e-Prime-Adv. Electr. Eng., Electron. Energy* **6**, 100308 (2023).
22. World Nuclear Association. Economics of nuclear power.https://world-nuclear.org/information-library/economic-aspects/economics-of-nuclear-power.aspx (2023).
23. Chatham House. The power of flexibility.https://www.chathamhouse.org/2018/08/power-flexibility/2-second-phase-transformations (2018).
24. International Energy Agency. United states 2024: Energy policy review. *Tech. Rep.*https://www.iea.org/reports/united-states-2024 (2024).
25. World Nuclear Association. Nuclear power in the usa.https://world-nuclear.org/information-library/country-profiles/countries-t-z/usa-nuclear-power.aspx (2024).
26. EIA. U.s. nuclear statistics.https://www.eia.gov/energyexplained/nuclear/data-and-statistics.php.
27. National Association of Regulatory Utility Commissioners (NARUC). Nuclear energy as a keystone clean energy resource. *Tech. Rep.*https://pubs.naruc.org/pub/5D91CEFD-1866-DAAC-99FB-768958414493 (2022).
28. U.S. Department of Energy. The ultimate fast facts guide to nuclear energy. *Tech. Rep.*https://www.energy.gov/sites/default/files/2024-02/ne-2023fastfactsguide-021424.pdf (2023).
29. U.S. Energy Information Administration. U.s. nuclear electricity generation continues to decline as more retirements occur.https://www.eia.gov/todayinenergy/detail.php?id=51978 (2021).
30. U.S. Energy Information Administration. First new u.s. nuclear reactor since 2016 is now in operation.https://www.eia.gov/todayinenergy/detail.php?id=57280 (2023).
31. Bockris, J. O. A hydrogen economy. *Science* **176**, 1323–1323 (1972).
32. U.S. Department of Energy, Office of Nuclear Energy. Nine mile point begins clean hydrogen production.https://www.energy.gov/ne/articles/nine-mile-point-begins-clean-hydrogen-production (2023).
33. Klevstrand, Agnete (Hydrogen Insight). Indispensable tool for climate — first nuclear hydrogen produced in the us at new york pilot project.https://www.hydrogeninsight.com/production/indispensable-tool-for-climate-first-nuclear-hydrogen-produced-in-the-us-at-new-york-pilot-project/2-1-1415744 (2023).
34. NucNet. U.s. initiative aims for production with nuclear — davis-besse project.https://www.nucnet.org/news/us-initiative-aims-for-productions-with-nuclear-energy-from-davis-besse-9-4-2022 (2022).
35. The White House. Biden-harris administration establishes bold u.s. government targets for safely and responsibly expanding u.s. nuclear energy.https://www.google.com/search?q=Biden%E2%80%93Harris%20Administration%20Establishes%20Bold%20U.S.%20Government%20Targets%20for%20Safely%20and%20Responsibly%20Expanding%20U.S.%20Nuclear%20Energy (2024).
36. L'Her, G., Kemp, R., Bazilian, M. & Deinert, M. Potential for small and micro modular reactors to electrify developing regions. *Nat. Energy* **9**, 725–734 (2024).
37. Vanatta, M., Patel, D., Allen, T., Cooper, D. & Craig, M. T. Technoeconomic analysis of small modular reactors decarbonizing industrial process heat. *Joule* **7**, 713–737 (2023).
38. NRC. Operating nuclear power reactors (by location or name).https://www.nrc.gov/info-finder/reactors/index.html (2025).
39. California Independent System Operator (CAISO). Caiso official website.https://www.caiso.com (2025).
40. Electric Reliability Council of Texas (ERCOT). Ercot official website.https://www.ercot.com (2025).
41. Midcontinent Independent System Operator (MISO). Miso official website.https://www.misoenergy.org (2025).
42. New York Independent System Operator (NYISO). Nyiso official website.https://www.nyiso.com (2025).
43. ISO New England. Iso-ne official website.https://www.iso-ne.com (2025).
44. Southwest Power Pool (SPP). Spp official website.https://www.spp.org (2025).
45. PJM Interconnection. Pjm official website. https://www.pjm.com (2025).
46. Bayramov, A. Comprehensive assessment of system efficiency and competitiveness of nuclear power plants in combination with hydrogen complex. *Int. J. Hydrog. Energy* **48**, 27068–27078 (2023).
47. Fernández-Arias, P., Vergara, D. & Orosa, J. A. A global review of pwr nuclear power plants. *Appl. Sci.* **10**, 4434 (2020).
48. EIA. Average retail price of electricity united states monthly https://www.eia.gov/electricity/data/browser/#/topic/7?agg=2,0,1&geo=g&freq=M&start=200101&end=202512&ctype=linechart&ltype=pin&rtype=s&maptype=0&rse=0&pin= (2026).
49. Mahmud, S. et al. A transactive energy framework for hydrogen production with economically viable nuclear power. In *Proceedings 2022 IEEE/PES transmission and distribution conference and exposition (T&D)*, 1–5 (IEEE, 2022).
50. Boardman, R. D., Westover, T. L., Remer, S. J. & Cadogan, J. Plan for scaling up hydrogen production with nuclear power plants. *Tech. Rep.* https://www.inl.gov/ (2022).

51. Fernández, L. J., Centeno, E. & Wogrin, S. Interactions between electricity and hydrogen markets: A bi-level equilibrium approach. *Int. J. Electr. Power Energy Syst.* **170**, 110902 (2025).
52. NREL. Annual technology baseline. https://atb.nrel.gov/ (2025).
53. Internal Revenue Service. Publication 946: How To Depreciate Property https://www.irs.gov/publications/p946 (2023).
54. Internal Revenue Service. Clean Electricity Investment Credit https://www.irs.gov/credits-deductions/clean-electricity-investment-credit (2024).
55. Internal Revenue Service. Clean Hydrogen Production Tax Credit (45V) Resources https://www.energy.gov/articles/clean-hydrogen-production-tax-credit-45v-resources (2024).
56. Wendt, D. S., Knighton, L. T. & Boardman, R. D. High temperature steam electrolysis process performance and cost estimates. *Tech. Rep.* https://doi.org/10.2172/1867883 (2022).
57. analytics, M. Mileage ratio issue. https://www.monitoringanalytics.com/reports/Presentations/2021/IMM_MRC_Mileage_Ratio_Issue_20210929.pdf (2021).
58. Tweed, K. Faster frequency regulation triples in pjm. https://www.greentechmedia.com/articles/read/faster-frequency-regulation-triples-in-pjm.(2025).
59. COMMISSION, F. E. R. Comments of the independent market monitor for pjm. https://www.monitoringanalytics.com/filings/2022/IMM_Comments_Docket_No_EL21-83_20221108.pdf. (2025).
60. CAISO. Informational report of the california independent system operator corporation. https://www.caiso.com/Documents/Jul31_2014_Order755MarketDesignReport_ER12-1630_ER14-971.pdf (2025).
61. Beacon Power, L. Overview of ferc order 755 and pay-for-performance regulation. https://www.ercot.com/files/docs/2014/03/19/regulation_pay_for_performance_032114.pdf (2025).
62. SPP. Re: Informational report of southwest power pool, inc. in dockets no. er13-1748-000 and er13-1748-001. https://www.spp.org/documents/37855/2016-05-02_informational%20report%20-%20order%20755%20compliance%20filing_er13-1748.pdf (2025).
63. Li, H. et al. Npph2: Code and data for "rethinking the economics and flexibility of u.s. nuclear power through hydrogen integration and policy support"https://doi.org/10.5281/zenodo.19646104 (2026).
64. International Energy Agency and Nuclear Energy Agency. Projected costs of generating electricity - 2020 edition. *Tech. Rep.*https://www.oecd-nea.org/upload/docs/application/pdf/2020-12/egc-2020_2020-12-09_18-26-46_781.pdf (2020).
65. OECD Nuclear Energy Agency. Unlocking reductions in the construction costs of nuclear: A practical guide for stakeholders. *Tech. Rep.*https://www.oecd.org/content/dam/oecd/en/publications/reports/2020/08/unlocking-reductions-in-the-construction-costs-of-nuclear_2ca6777b/33ba86e1-en.pdf (2020).
66. International Atomic Energy Agency. Nuclear power capacity trend (2005-2024).https://pris.iaea.org/pris/worldstatistics/worldtrendnuclearpowercapacity.aspx (2025).
67. World Nuclear Association. World nuclear performance report 2024 https://world-nuclear.org/our-association/publications/world-nuclear-performance-report.aspx (2024).

Acknowledgements

This manuscript has been authored in part by a contractor of the U.S. Government under the U.S. Department of Energy, Office of Nuclear Energy, Idaho Operations Office Contract No. DE-AC07-05ID14517. By accepting the article for publication, the publisher acknowledges that the U.S. Government retains a nonexclusive, paid-up, irrevocable, worldwide license to publish or reproduce the published form of this manuscript, or to allow others to do so, for U.S. Government purposes.

Author contributions

H.L., J.H., B.P. and J.Z. conceived the study and designed the methodology. H.L., J.H. and B.P. carried out the modeling and analyses. H.L., B.P., T.W. and D.W. contributed resources. H.L. wrote the original draft. H.L., J.H., B.P., T.W. and J.Z. reviewed and edited the manuscript. B.P., M.S. and J.Z. supervised the work. J.Z. acquired funding.

Funding

J.Z. acknowledges support from the U.S. National Science Foundation under Grant No. 2229417 and the Hydrogen INTERN program.

Competing interests

The authors declare no competing interests.

Additional information

Supplementary information The online version contains supplementary material available at https://doi.org/10.1038/s41467-026-73630-y.

Correspondence and requests for materials should be addressed to Jie Zhang.

Peer review information *Nature Communications* thanks Machiel Mulder and the other anonymous reviewer(s) for their contribution to the peer review of this work. A peer review file is available.

Reprints and permissions information is available at http://www.nature.com/reprints

Publisher's note Springer Nature remains neutral with regard to jurisdictional claims in published maps and institutional affiliations.

Open Access This article is licensed under a Creative Commons Attribution-NonCommercial-NoDerivatives 4.0 International License, which permits any non-commercial use, sharing, distribution and reproduction in any medium or format, as long as you give appropriate credit to the original author(s) and the source, provide a link to the Creative Commons licence, and indicate if you modified the licensed material. You do not have permission under this licence to share adapted material derived from this article or parts of it. The images or other third party material in this article are included in the article's Creative Commons licence, unless indicated otherwise in a credit line to the material. If material is not included in the article's Creative Commons licence and your intended use is not permitted by statutory regulation or exceeds the permitted use, you will need to obtain permission directly from the copyright holder. To view a copy of this licence, visit http://creativecommons.org/licenses/by-nc-nd/4.0/.

© The Author(s) 2026